ESTIMATION OF AIRFRAME DRAG BY SUMMATION OF COMPONENTS: PRINCIPLES AND EXAMPLES

1. NOTATION AND UNITS

There is no subdivision of aircraft drag or drag coefficient for which a single set of terms or notation exists. This is true generally and within the many drag-related ESDU Data Items. Since the present Item is intended to deal with the overall estimation of drag and its relationship to other Items (and other sources) some general principles have been adopted.

For convenience, most of the text and many of the equations *in this Data Item* are expressed in terms of drag rather than drag coefficient so as to simplify the notation used.

Capital letter subscripts to drag, D, indicate a drag contribution related to a particular flow mechanism.

Lower case word subscripts (or abbreviations) to drag, D, indicate a drag contribution due to a particular airframe component or flight condition.

Notation used once only in any of Tables 6.2 to 6.10 is defined there and not included here.

		SI	*British*
A	aspect ratio, b^2/S		
a	speed of sound	m/s	ft/s
b	wing span	m	ft
C_D	drag coefficient, D/qS		
C_{D_F}	drag coefficient due to skin friction, D_F/qS		
$C_{D_{min}}$	minimum value of C_D at given value of M		
C_{D_P}	profile drag coefficient, D_P/qS		
$C_{D_{PR}}$	pressure drag coefficient, D_{PR}/qS		
$C_{D_{TV}}$	trailing vortex drag coefficient, D_{TV}/qS		
C_{D_V}	viscous drag coefficient, D_V/qS		
C_{D_W}	wave drag coefficient, D_W/qS		
C_F	flat plate mean skin friction coefficient		

C_{F_e}	equivalent skin friction coefficient, = (aeroplane drag component independent of lift)/qS_{wet}		
C_f	flat plate local skin friction coefficient		
C_L	lift coefficient, L/qS		
$C_{L_{crit}}$	"critical" value of C_L in "dual parabolic" representation of drag polar		
C_p	pressure coefficient (= $(p_{local}-p)/q$)		
c	chord of aerofoil or of wing at spanwise station η	m	ft
$\bar{c}$	wing geometric mean chord	m	ft
D	drag	N	lbf
$D_{asym\ thr}$	drag due to thrust asymmetry	N	lbf
D_F	drag due to skin friction	N	lbf
D_i	lift-dependent component of drag	N	lbf
D_P	profile drag	N	lbf
D_{P_n}	profile drag of strip normal to wing sweep line	N	lbf
D_{P_s}	profile drag of streamwise strip of wing	N	lbf
D_{PR}	pressure drag	N	lbf
D_{stores}	stores drag (*e.g.* fuel tanks, weapons)	N	lbf
D_{TV}	trailing vortex drag	N	lbf
D_{trim}	longitudinal trim drag	N	lbf
D_{uc}	undercarriage drag	N	lbf
D_V	viscous drag	N	lbf
D_W	wave drag	N	lbf
D_0	component of drag independent of lift	N	lbf
d	maximum diameter of body (or of equivalent axisymmetric body) of aircraft or of component indicated by subscript	m	ft
e	efficiency factor		

f	denotes function of form, f[…]		
g	acceleration due to gravity	m/s^2	ft/s^2
j	denotes jth strip of wing or other aerodynamic surface		
K, K_1, K_2	lift-dependent drag factors		
L	lift	N	lbf
l	characteristic length	m	ft
M	Mach number, V/a		
mfr	intake mass flow ratio		
N	number of chordwise strips used to represent wing between root and tip		
p	static (ambient) pressure in free stream	N/m^2	lbf/ft^2
p_{local}	local surface pressure on airframe	N/m^2	lbf/ft^2
q	kinetic pressure, $\rho V^2/2$ (identical to dynamic pressure in incompressible flow)	N/m^2	lbf/ft^2
Re	Reynolds number, $\rho Vl/\mu$		
S	wing reference area	m^2	ft^2
S_{wet}	wetted area of aircraft or component indicated by subscript	m^2	ft^2
t	maximum thickness of aerofoil or wing	m	ft
V	true airspeed	m/s	ft/s
x, y, z	coordinates, parallel to aircraft body axis system but with origin chosen to suite the particular topic	m	ft
Δ	denotes an increment in the affixed parameter		
$(1 + \delta)$	lift dependent drag factor due to wing trailing vortices (Reference 26)		
η	non-dimensional spanwise coordinate, $y/(b/2)$		
Λ	sweep of wing	deg	deg
Λ_e	equivalent sweep angle of wing, see Table 6.9	deg	deg
λ	form factor		
μ	dynamic viscosity	N s/m^2	lbf s/ft^2
ρ	density of air	kg/m^3	$slug/ft^3$

Subscripts

D	denotes drag-rise condition
$datum$	denotes datum value of parameter
j	denotes value for jth strip of wing or other aerodynamic surface
min	denotes minimum value
n	denotes quantity defined in plane containing equivalent two-dimensional aerofoil (see Section 3.3.2.1)
s	denotes quantity defined in streamwise plane parallel to (wing) plane of symmetry
$tail$	denotes tail
$trim$	denotes (longitudinal) trimmed condition
wb	denotes value for wing-body combination
ΔC_L	denotes change in a parameter due to change, ΔC_L, in C_L
ΔM	denotes change in a parameter due to change, ΔM, in M
ΔRe	denotes change in a parameter due to change, ΔRe, in Re
¼ , ½	denotes values at wing quarter chord and half chord locations
0	denotes (i) conditions at sea level in ISA (ii) drag component independent of lift

2. INTRODUCTION

Most airframe drag estimation methods* rely on the summation of contributions due to particular airframe components or flow mechanisms. Examples of several schemes are given and one of these (Table 6.5) presents the basis of the drag estimation method of Reference 49.

Section 3 itemises contributions to overall airframe drag that should, ideally, be considered – although with some procedures two or more of those items are coalesced. Section 4 reviews the practicalities of making these estimates and Table 6.11 lists the ESDU data available.

An introduction to the *representation* of airframe drag for performance calculations is given in Data Item No. 81026 (Reference 32) together with examples of individual aircraft drag characteristics.

The examples of drag estimation schemes considered here in Tables 6.2 to 6.10 range from the relatively simple to those that require at least some usage of CFD techniques. The former tend to be the oldest and probably the most amenable to use at an early stage in design where limited geometric information is available. The latter are more representative of drag estimation procedures in current use wherever CFD techniques are the mainstay of (wing) aerodynamic design. The further that a project proceeds to wind-tunnel and, eventually, flight testing, the more likely the process of drag prediction and correlation will involve a mixture of all available techniques*.

* This Item does not address the following
(1) The derivation of whole-airframe drag from the adjustment of wind-tunnel measurements to full scale.
(2) The estimation of drag from the use of CFD simulation of the complete airframe.

3. REFERENCE SCHEME FOR DRAG CONTRIBUTIONS

A recurrent problem with drag estimation/analysis procedures is the number of ways of subdividing the total drag, the level of detail to which the various contributions to drag are addressed and the nomenclature/notation used.

Sketch 3.1 shows how drag can be subdivided in several ways. In particular, it shows the interaction between schemes based on fluid-flow principles and those based on the principle of conservation of momentum. All drag estimation methods can be related to Sketch 3.1, but there are many ways of further subdividing the drag and of predicting individual terms – especially when airframe components are considered separately.

This Data Item presents, in summary form, several existing drag estimation methods so as to illustrate, by example, the range of techniques and levels of sophistication that exist. To provide a common format for those Examples, a Reference Scheme and associated Notation is presented as Table 6.1. Subsequently, Tables 6.2 to 6.10 give the individual examples.

Sections 3.1 to 3.9 provide commentaries on the individual items in the Reference Scheme. Note that some of the Examples in Tables 6.2 to 6.10 do not consider the whole airframe. In other cases two (or more) items of the Reference Scheme may be coalesced into a single drag contribution.

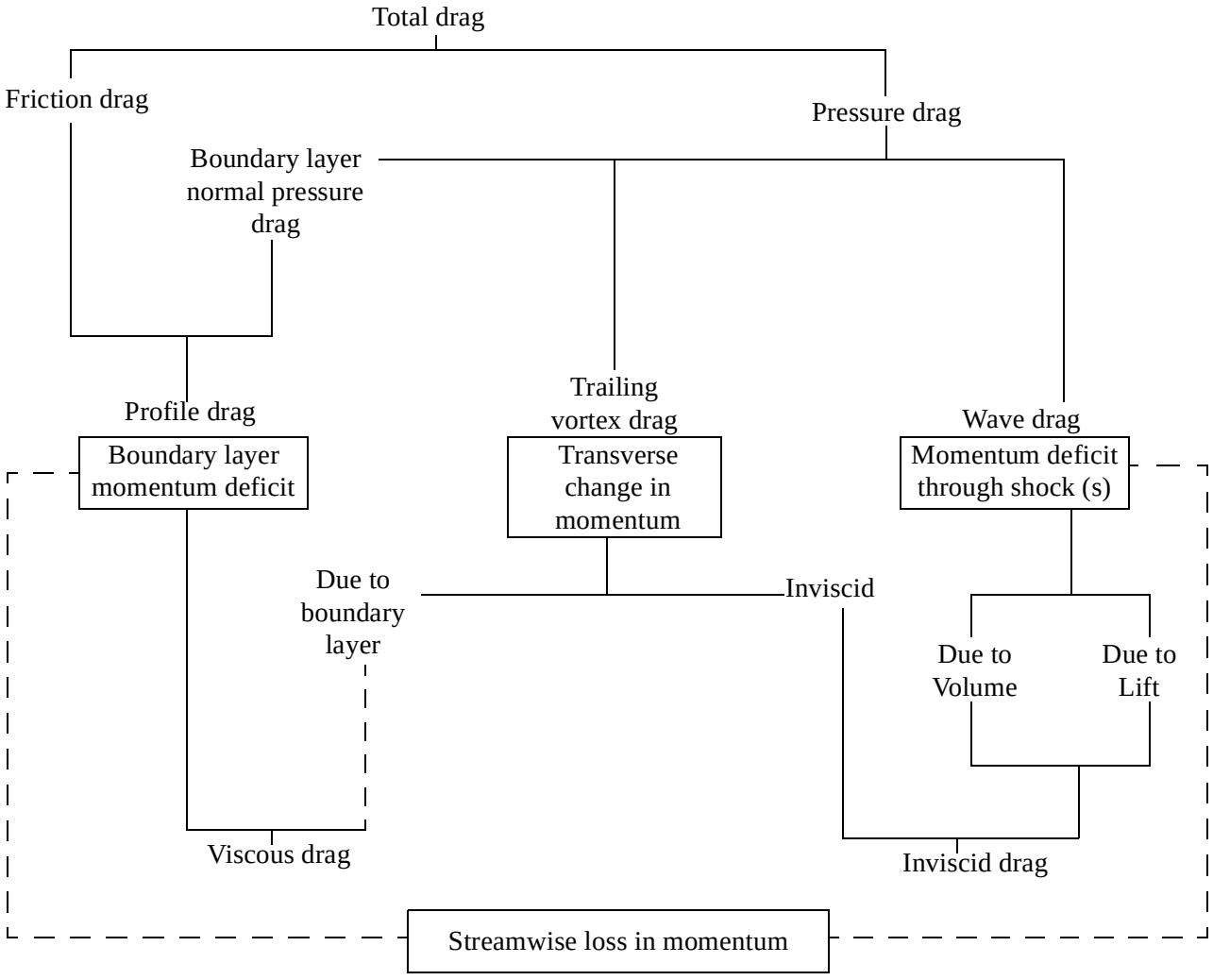

Sketch 3.1 Relationship Between Drag, Drag Components And Momentum Changes

3.1 Total Drag

The Reference Scheme of Table 6.1 is presented in terms of contributions to total drag, D, rather than to the total drag coefficient, C_D. This simplifies the notation and acknowledges that some contributions are not best represented by parameters which include the aircraft reference area.

For each of the examples in Tables 6.2 to 6.10 the notation column remains the same as in the Reference Scheme. The summary of the method given in each Table reflects the terminology of that method but, where symbols are required, uses those of the Reference Scheme wherever possible.

3.2 Datum Conditions for Airframe Drag

The purpose of datum conditions in a drag estimation method is to allow the complete calculation to be performed at those conditions while incremental adjustments are used to generate estimates away from the datum. The use of computational procedures might be thought to render such an approach unnecessary but even here it can be advantageous. For example, it permits the use of data of high quality but limited extent in the region of the datum conditions while accepting that the adjustments to off-datum conditions might be less well founded. The approach is useful also in describing methods (as here) and in identifying the source of small changes in estimated drag for different flight conditions.

If used, the datum conditions consist of some combination of values of C_L, M, Re.

Datum lift coefficient: The traditional approach to profile drag estimation puts $C_{Ldatum} = 0$. However, when considered in terms of airframe aerodynamics, this is not a condition of particular significance and for many aircraft is not a realistic flight condition. Consequently, some methods are formulated around values of C_{Ldatum} (and M_{datum}, see below) which correspond to some optimum feature of aerofoil and/or wing aerodynamics.

Datum Mach number: The desire to simplify skin-friction calculations (by using a single value of Reynolds number) might lead to M_{datum} being taken as a cruise value. Alternatively, a value might be selected at which no wave drag would occur at any flight conditions. A further option is to use datum values of C_L and M which correspond to some optimum feature of aerofoil and/or wing aerodynamics. Examples are combinations of C_L and M which correspond to

(i) a wing design point (see Reference 47 for review of these),

(ii) maximum value of ML/D (Table 6.5 provides an example),

(iii) the drag-rise condition for some specified standard of wing/aerofoil design (Table 6.9 provides an example).

Datum Reynolds number: Skin-friction calculations can be simplified by taking nominal values of C_F at a single datum value of Reynolds number for each airframe component. Adjustments to other conditions can then be made by a simple factor – as illustrated in Addenda B and D of Reference 32. The datum might be taken as a cruise condition or to correspond with other datum conditions.

3.3 Profile Drag

Profile drag is generally regarded as the drag arising due to the presence of the boundary layer on any object moving through a fluid – see Sketch 3.1. This definition allows for the variation in profile drag with lift coefficient (or angle of attack) due to the effect on the boundary layer of changes in the surface pressure distribution. For some estimation procedures the term has come to include the contribution due to wave drag at subsonic speeds. Methods in use for major airframe components, especially wings, are considered in Sections 3.3.1 to 3.3.3. General remarks regarding the contributions due to excrescences, interferences and propulsion systems are given in Sections 3.3.4 to 3.3.6.

3.3.1 Use of flat plate skin friction and form factors

For attached flow on smooth and uniformly rough surfaces, the traditional approach to profile drag estimation is to divide the airframe into a convenient set of j components, say, and to evaluate the sum of their drag contributions as

$$D_p = \sum_{j=1}^{N} [D_p]_j = q \sum_{j=1}^{N} [S_{wet} \times C_F \times \lambda]_j . \qquad (3.1)$$

Thus, for each airframe component it is necessary to estimate a value for:

S_{wet} the wetted area of the component,

C_F the flat plate mean skin friction coefficient, estimated at a Reynolds number based on an appropriate streamwise dimension,

λ the "form factor" for the component, *i.e.* the ratio of the drag to the drag of a flat plate with the same Reynolds number and transition position.

In using Equation (3.1) systematic errors can be avoided if it is ensured that values of C_F and S_{wet} are based on the same skin friction law and wetted area definition as was used in the derivation of the values of λ. For example, is the "flat plate" area the true surface area of the component or (for a wing, tail, pylon *etc.*) simply twice the planform area? If the latter approach is used, then the effects on surface area of thickness and of dihedral/anhedral are omitted from the calculation.

For some airframe components the use of single values of C_F and λ (even if they are "equivalent" ones) is overly simplistic; in the case of wings and other lifting surfaces this restriction leads to the use of the "strip" methods introduced in Section 3.3.2.

3.3.2 Profile drag estimation using strip methods and simple sweep rules

Strip methods, taken together with the simple sweep rules for an infinite swept wing, provide a means of using two-dimensional aerofoil data to predict profile drag of wings. The approach adopted here is to provide a review of the sweep rules in Section 3.3.2.1 and to give general guidance on the use of strip methods in Section 3.3.2.2. Particular applications are mentioned in Tables 6.3, 6.5, 6.8, 6.9.

3.3.2.1 Simple sweep rules

This section is adapted from Section 5 of Reference 40.

On an unswept wing the flow departs from a two-dimensional character only close to the wing tips, where the formation of tip vortices causes three-dimensional features in the boundary layer and external flow. Wings of moderate sweep (about 30 degrees, say) and high aspect ratios typical of most modern transport aircraft, are often designed so that the flow (except in regions near the roots and tips) is of a quasi-two-dimensional nature, in the sense that it varies only slowly across the span. In these 'mid-semi-span' regions the idealised concept of an 'infinite yawed wing' is a useful starting point, which relates the swept-wing flow to an equivalent two-dimensional flow over a transformed aerofoil section, taken normal to the leading edge of the actual wing, see Sketch 3.2.

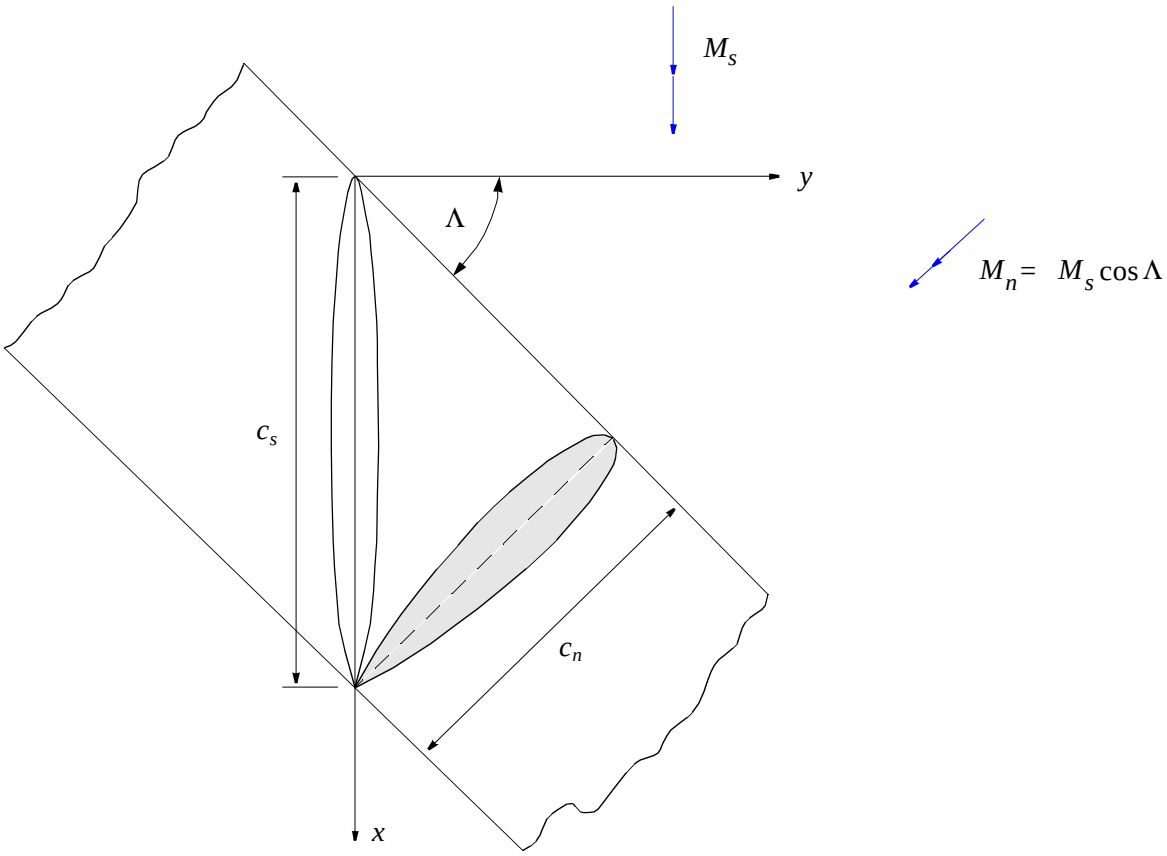

Sketch 3.2 Illustration of transformed aerofoil

Following the notation illustrated in Sketch 3.2 and using "*s*" to denote streamwise conditions and "*n*" to denote equivalent-two-dimensional conditions, the following relationships may be derived.

From geometric considerations

$$c_n = c_s \cos\Lambda ,$$
$$z_n = z_s ,$$

so
$$\left(\frac{z}{c}\right)_n = \left(\frac{z}{c}\right)_s \sec\Lambda \tag{3.2}$$

and
$$\left(\frac{t}{c}\right)_n = \left(\frac{t}{c}\right)_s \sec\Lambda . \tag{3.3}$$

From the aerodynamics of the two flow cases,

$$M_n = M_s \cos\Lambda , \tag{3.4}$$
$$V_n = V_s \cos\Lambda . \tag{3.5}$$

Since, for an infinite wing, the pressure perturbations, $(p_{local} - p)$, are the same in the two flow cases, as are p and ρ, it follows that

$$\frac{(p_{local} - p)}{\frac{1}{2}\rho V_n^2} = \frac{(p_{local} - p)\sec^2\Lambda}{\frac{1}{2}\rho V_s^2}$$

or
$$[C_p]_n = [C_p]_s \sec^2\Lambda . \tag{3.6}$$

Since values of lift coefficient are obtained by integration of the values of C_p around the aerofoil, it follows from Equation (3.6) that the lift coefficients of the two flows are related by

$$[C_L]_n = [C_L]_s \sec^2\Lambda \tag{3.7}$$

while, because of Equations (3.2) and (3.3), the pressure drag coefficients are related by

$$[C_{D_{PR}}]_n = [C_{D_{PR}}]_s \sec^3\Lambda . \tag{3.8}$$

These equations are strictly true only for inviscid flow – no such simple relationships are valid for the viscous drag, particularly when the boundary layers are turbulent – but they are still useful as a general overall guide. In particular, since wave drag is a mainly inviscid phenomenon, the wave drag coefficients are related by

$$[C_{D_W}]_n = [C_{D_W}]_s \sec^3\Lambda . \tag{3.9}$$

Thus the flow on a swept wing of sweep angle Λ may be compared with the flow on an equivalent aerofoil which is thicker (factor, $\sec\Lambda$), at a higher lift coefficient (factor, $\sec^2\Lambda$) and at a lower free-stream Mach number (factor, $\cos\Lambda$). (The beneficial effect of sweep is due to the fact that the last of these three factors generally easily outweighs the adverse effects of the other two. In particular, the appearance of shock waves, and their consequent adverse effects on the development of drag and separation, is progressively delayed as the sweep angle is increased.)

3.3.2.2 Strip methods

The principle is that profile drag of a swept tapered wing is estimated by dividing the wing into a number (j, say) of strips – both "streamwise" (subscript "s") and "normal" (subscript "n") to the wing sweep line, however defined. For each strip it is assumed that the geometry (chord, thickness, sweep) and flow conditions are constant, or effectively so.

For the required conditions of Mach number, M, and wing lift coefficient, C_L, spanwise loading data are used to determine the lift coefficient, $C_{L_{s,j}}$, for each strip. For this purpose the condition $C_L = 0$ represents a trivial case while the simplest procedure with $C_L \neq 0$ is to assume an elliptical spanwise variation of loading and hence of $C_{L_{s,j}}$.

Geometry and flow conditions for the equivalent two-dimensional aerofoil sections are derived as follows.

Equations (3.2) and (3.3) give the co-ordinates and thickness, $[z/c]_{n,j}$ and $[t/c]_{n,j}$,

Equation (3.4) gives the Mach number $M_{n,j}$,

Equation (3.7) gives the lift coefficient $C_{L_{n,j}}$.

Ideally, values of pressure drag coefficient are obtained for the transformed aerofoil and flow conditions for each strip and converted into an estimate of wing profile drag using Equation (3.8) and the summation,

$$D_P = q \sum_{j=1}^{N} S_j \left[C_{D_{F_s}} + C_{D_{PR_n}} \cos^3 \Lambda \right]_j . \tag{3.10}$$

In Equation (3.10) $C_{D_{Fs,j}}$ is evaluated for *streamwise* flow conditions. The need to select several values of Λ arises in the examples of Tables 6.3, 6.4, 6.8 and 6.9. In Table 6.3 the value of $\Lambda_{¼}$ for the wing is used. In Table 6.4 the method of Reference 6 calls for the use of Λ values for each percentage chord line in deriving co-ordinates of the equivalent two-dimensional sections. Table 6.8 suggests the use of either $\Lambda_{¼}$ or $\Lambda_{½}$ for the wing. Table 6.9 makes use of the values of an effective sweep angle, Λ_e, derived and presented in Data Item No. 72027 (Reference 25). Other forms of Equation (3.10) may have to be used – depending on the type of aerofoil data available. In the most general case, with values of aerofoil profile and wave drag coefficients given separately,

$$D_P = q \sum_{j=1}^{N} S_j \left[C_{D_{F_s}} + \left[C_{D_{W_n}} + \left(C_{D_{P_n}} - C_{D_{F_s}} \right) \right] \cos^3 \Lambda \right]_j . \tag{3.11}$$

In the simplest case, where there is no wave drag and aerofoil profile drag is expressed in terms of form factors (see Section 3.3.1), Equation (3.11) becomes

$$D_P = q \sum_{j=1}^{N} S_j C_{F_{s,j}} [1 + (\lambda_n - 1) \cos^3 \Lambda]_j . \tag{3.12}$$

Again, in Equations (3.11) and (3.12) values of $C_{D_{F_{s,j}}}$ and $C_{F_{s,j}}$ are determined based on streamwise flow conditions.

Equation (3.12) can be represented in a form which relates purely to quantities defined in the streamwise direction, as follows. Since for most aerofoils $(\lambda - 1)$ is a linear function of t/c as long as attached-flow conditions prevail then, from Equation (3.3),

$$(\lambda_n - 1) = (\lambda_s - 1)\sec\Lambda . \tag{3.13}$$

Combining Equations (3.12) and (3.13) gives

$$D_P = q \sum_{j=1}^{N} S_j C_{F_{s,j}} [1 + (\lambda_s - 1)\cos^2\Lambda]_j . \tag{3.14}$$

The use of strip methods is limited to cases where the assumption of quasi-two-dimensional flow over much of the wing is reasonable. This can be interpreted as restricting the methods to aspect ratios greater than about 3 and sweep angles less than about 45 deg.

3.3.3 Profile drag estimation using full boundary-layer calculations

In principle, any analytical or numerical method of representing boundary-layer development can lead to a method for profile drag prediction – see for example, References 1 to 5, and 3.

The "verification" Sections 7.1.2 and 7.2.2 of Data Item No. 87003 (Reference 38) include examples of the successful application of a full three-dimensional boundary-layer method to calculation of profile drag for both a high and a low aspect ratio wing – see Table 6.10.

3.3.4 Excrescence drag

Excrescence drag estimation methods range from some crude fraction of the profile drag "without excrescences" to detailed calculations following a complete survey of the airframe as-built. Data Items in the ESDU Aerodynamics Series are appropriate in the latter case – see Table 6.11. More approximate but quicker estimates are provided by the methods given in Data Item No. 94044 (Reference 42). The definition given in that Item, and adopted here, is as follows, *"anything other than distributed (or "sand grain") roughness that appears on the aircraft but is not represented on a wind-tunnel model or equivalent theoretical model"*. Reference 42 treats each of the following categories of excrescences:

airframe-build surface imperfections,
imperfections associated with movable aerodynamic surfaces,
air data sensors,
lights and beacons,
antennae,
static discharge wicks,
rain dispersal: screen wipers/blowing/fluid; gutters over doors,
drains,
fuel system,
ventilation/cooling,
air conditioning/pressurisation,
auxiliary power unit.

A few other miscellaneous items are considered in Reference 42 but the following are *excluded*,

vortex generators (see Data Item Nos 93024, 93025), fences,
flap tracks, engine/stores pylons,
thrust reversers,
refuelling probe.

3.3.5 Interference drag

Aerodynamic interference between adjacent airframe components is inevitable because of the coalescing of the pressure fields of the individual components and the confluence of their boundary layers in junction regions. Such interferences are not, necessarily, detrimental and in some cases "favourable" results are obtained by the detailed shaping of components. Most of the drag estimation methods in Tables 6.1 to 6.9 assume that interferences are either small (or negligible, or "curable") or can be dealt with by simple methods*. Those Tables include references to such methods for interferences between

wing/body,
wing/pylon/nacelle,
wing/flap tracks,
tail/body/nacelle,
fin/body,
fin/tail.

3.3.6 Propulsion system drag terms

The convention regarding forces associated with the external flow (*i.e*. drag and lift) and the internal-flow stream tube (*i.e*. thrust) of turbo-jet and turbo-fan engines is assumed to be as defined in Item No. 69006 (Reference 21; see also Reference 10). In the case of propeller-driven aircraft References 36 and 37 give guidance on thrust and drag accounting while Addendum F of Reference 32 gives an example for a large turbo-prop aircraft.

Most of the methods in Tables 6.2 to 6.10 do not include treatment of these terms, primarily because they are viewed as "off-design" cases. For situations where they have to be considered, the main items are as follows.

Intake spillage drag, is the *change* in drag (by definition, in the external flow) associated with a change in intake operating conditions from some chosen datum. A change in intake operating conditions occurs whenever the powerplant demand for air (*i.e*. the internal flow) changes and is characterised by values of the intake *mass flow ratio*, *mfr*. For a simple pilot intake the condition *mfr* = 1.0 (intake running full) is often used as the datum for spillage-drag calculations. Values of *mfr* < 1.0 then imply that air "spills" around the intake lip with consequent effects on drag due to:

(i) increased (attached) flow velocities on the intake external surface,

(ii) flow separation on the intake lip,

(iii) shock wave development on the intake external surface.

Items (i) and (ii) are treated in References 34 and 33 while item (iii) is dealt with in Reference 41.

* The full simulation of such effects, either by Computational Fluid Dynamics (CFD) techniques or by wind-tunnel testing is outside the scope of this Data Item.

It follows from the thrust definitions of References 21 and 10 that the drag of an intake (or cowl forebody) *at each value of mfr* is made up of the following contributions.

[Drag of intake (or cowl forebody]	=	[Pre-entry force on external surface of entry stream tube]	+	[Streamwise force on intake (or cowl forebody)]
(Positive in all real flows)		(Positive contribution to drag calculation, References 34 and 41 give values)		(Negative contribution to drag calculation, *i.e.* suction on intake lip and forebody).

Therefore, the estimation of a single value of spillage drag implies, in principle, the evaluation of the above expression at the chosen datum value of *mfr* and at the *mfr* value of interest.

Afterbody and base drag contributions appear in the methods in Tables 6.2, 6.4 and 6.7 and are dealt with in several Data Items in the ESDU Aerodynamics Series – See Table 6.11. The most usual method for dealing with the effects of engine exhaust jet flow is to treat the nozzle pressure ratio as an independent variable with a datum value chosen to correspond with some convenient engine operating condition.

For subsonic transport aircraft at normal cruise conditions (all engines operating), little or no effect of spillage drag or afterbody or base drag is to be expected. For supersonic aircraft, spillage drag increments can be reduced by the use of variable geometry intake systems. Where these effects are considered in detail, airframe drag is calculated initially for the datum values of those variables, such as intake mass flow ratio and nozzle pressure ratio, used to describe the propulsion system flow conditions (see, for example, Addendum G in Reference 32). Values of spillage drag and of afterbody or base drag can then be added to correspond with any chosen engine operating conditions. Note that there is no reason for the intake and exhaust datum flow conditions to be consistent with one another – indeed it would be difficult to make them so.

Windmilling (or "locked-rotor") drag for jet and fan engines is dealt with in Reference 31 while Reference 35 addresses the combined use of References 31 and 34. Drag of **windmilling propellers** is addressed in Reference 20.

Drag due to asymmetric flight, associated with an inoperative powerplant or airframe asymmetry, is the subject of Reference 39.

3.4 Effect on Profile Drag of Changes in C_L, M, Re

Skin friction varies systematically with M and Re so that if profile drag is evaluated at datum values of these parameters, there will be changes in D_P when the values of M and Re change from the datum. An example is given in Addendum B of Reference 32.

Profile drag changes with change in C_L (or angle of attack) and those changes can be estimated using the methods described in Section 3.3.2 and 3.3.3. In some methods, however, the variation of D_P with C_L is treated as part of the overall "lift dependent drag" – in which cases it is assigned to items (5) and (6) in Table 6.1.

Changes in Mach number, at constant C_L, can lead to small variations in D_P due to their effects on the overall pressure distribution (sub-critical "drag creep"). The onset of shock waves and the associated wave drag clearly is a function of Mach number although at subsonic speeds this may be assigned to profile drag as a matter of convenience.

3.5 Trailing Vortex Drag

For attached flow on planar wings with elliptic loading, the trailing vortex drag is well predicted using

$$C_{D_{TV}} = \frac{C_L^2}{\pi A}. \tag{3.15}$$

To cope with departures from these ideal conditions Equation (3.15) is often modified to

$$C_{D_{TV}} = \frac{C_L^2(1+\delta)}{\pi A}. \tag{3.16}$$

Values of $(1+\delta)$ to take account of the effects of sweep and taper in subcritical, compressible potential flow for planar wings are given in Data Item No. 74035 (Reference 26).

To deal, approximately, with the effect of the body on wing spanwise loading, and hence on trailing vortex drag, several methods, including that of Table 6.2, make $C_{D_{TV}}$ a function of the ratio of body diameter to wing span.

To determine completely the vortex drag of a wing requires a knowledge of the spanwise load distribution, including any influences of the boundary layer. The example in Table 6.10 is based on such a method.

For separated flow cases $C_{D_{TV}}$ may be represented as a linear function of $(C_L^2 - C_{L_{crit}}^2)$ as in Table 6.7 and Reference 32, Addendum D. Estimation of vortex drag in this flow regime is the subject of Data Item Nos 95025 and 96025 (References 43 and 46).

3.5.1 Combination of trailing vortex drag and lift-dependent profile drag

Much use has been made of factors K or e to allow *all* lift-dependent drag contributions to be combined into a single expression such as

$$C_{D_i} = \frac{KC_L^2}{\pi A} \text{ or } \frac{C_L^2}{\pi eA}. \tag{3.17}$$

The factors K and e in Equation (3.17) thus have to account not only for any effects of non-elliptic loading on the vortex drag but for all aspects of profile drag variation with lift. No genuine estimation method exists for the values of K or e as defined in Equation (3.17), but the methods in Tables 6.2 and 6.6 make use of values based on previous experience.

3.6 Effects on Trailing Vortex Drag of Changes in C_L, M, Re

The effect of changes in lift coefficient follow directly from the methods described in Section 3.5. Effects of Mach number and Reynolds number are unlikely to be seen, except when using the most detailed prediction methods – the method considered in Table 6.10 is one such example.

3.7 Wave Drag

At subsonic flight speeds, shock waves signify the abrupt termination of local regions of supersonic flow. The shock wave locations and strengths depend on surface geometry and vary with Mach number and incidence (see Reference 40). The situation is further complicated if the shock strength is sufficient to cause separation of the boundary layer.

The methods described in Tables 6.2, 6.3, 6.4, 6.6 and 6.7* rely on one or other means of predicting a drag-rise Mach number at or above which a fixed increment in, or standard variation of, drag coefficient is presumed. The method of Table 6.5* is empirical – based on the principles of transonic similarity – and predicts drag coefficient variations with M and C_L about a pre-determined datum. An introduction to the rules of subsonic, transonic and supersonic similarity is given in Reference 48. The only methods included here that provide systematic means of predicting wave drag (of wings) are those in Tables 6.9 and 6.10. The former of these requires the use of aerofoil data at the drag rise conditions and a CFD code to examine variations from that condition. (A similar procedure for the drag rise condition alone is involved in Table 6.4). The method of Table 6.10 requires a detailed knowledge of the pressure distribution on the wing surface so that the shock strength and position can be identified.

A further method for dealing with wave drag at subsonic speeds, but requiring detailed information for an existing airframe, is given in Reference 27.

For forebodies and axisymmetric forecowls values of wave drag at $M<1$ are included in the Items listed in Table 6.1.

At supersonic flight speeds the presence of a bow shock makes systematic calculations of wave drag more practicable – see Table 6.11, for example. The methods described in Tables 6.5 and 6.7 each provide estimates of wave drag at supersonic speeds although in the method of Table 6.5 the procedure used does not immediately allow values of D_W to be deduced.

3.8 Longitudinal Trim Drag

Longitudinal trim drag comprises those additional drag contributions associated with maintaining zero† resultant moment about the aircraft pitch axis. Such contributions arise in both steady level flight (zero *pitch rate*) and in any manoeuvre (turn, loop, pull-up) where a constant pitch rate is maintained.

(This terminology differs from that customarily used in flight-dynamics work – where the trimmed condition is one in which the control system is set so as to leave zero force on the pilot's longitudinal control lever. The two definitions are identical only in the case where longitudinal control is achieved with a single surface serving as both stabiliser and control in which case the pilot's act of "trimming" implies the zeroing of an artificial-feel system.)

The evaluation of longitudinal trim drag can take many routes and, since the full process is iterative, the main elements are described in Sections 3.8.1 to 3.8.3 in general terms only. Section 3.8.4 presents several options for defining the aircraft "datum trim condition" and indicates some of the consequences of each.

Throughout Sections 3.8.1 to 3.8.4 it is presumed that the aircraft configuration is one where longitudinal control/trim are achieved with a horizontal tailplane (with or without moveable surfaces). Section 3.8.5 considers briefly the case of foreplanes and "close-coupled" control/trim surfaces.

---

* Tables 6.5 and 6.7 deal with subsonic and supersonic flight cases.

† A non-zero resultant moment in pitch, as in initiation/termination of a pitching manoeuvre, could be considered but the effect on *drag* is likely to be small.

3.8.1 Lift on wing and tailplane

For a given aircraft lift requirement the division of lift between the wing and tailplane is calculated by setting the resultant pitching moment on the aircraft to zero. For some aircraft this includes the possibility for favourable movement of the centre of gravity position if fuel can be transferred between fore and aft tanks. Downwash effects and any thrust component in the lift direction must be accounted for while the aircraft lift is held constant.

3.8.2 Downwash

A knowledge of the mean downwash at the tailplane is a prerequisite to all the calculations, so that

forces required of the tailplane can be related to the relevant aerodynamic data,

forces produced by the tailplane can be resolved into components in the aircraft lift and drag directions.

Values of downwash are dependent on configuration (including undercarriage and airbrake positions and "stores" carried) and lift and in some cases on powerplant setting.

3.8.3 Drag increments

In principle, provided the aerodynamic data are available, drag values can be deduced for any division of lift between the wing and tailplane.

Changes in wing drag due to change in wing lift are calculated in the usual way.

For a fixed tailplane with a movable elevator, and for a variable-incidence tailplane with no elevator, there is a unique deflection to produce the required lift and so a unique value of drag. (The second of these configurations is typical of many combat aircraft types and an example is provided in Addendum G of Reference 32.)

For a variable-incidence tailplane *with an elevator* there is a range of configurations yielding the required lift force and a corresponding range of drag values. Lower and upper limits are provided as follows.

Tailplane angle to trim at zero elevator deflection; this is the case of primary interest for many transport aircraft in cruise.

Elevator angle to trim at fixed tailplane angle, corresponding to the situation in manoeuvring flight.

3.8.4 Datum trim conditions

Because of the need to ensure that the longitudinal trim drag is correctly accounted for and because it arises from "existing" airframe components, the concept of datum trim conditions is sometimes used. Examples of the effect of this approach on the contributions to D_{trim} are as follows.

$$D_{trim} = \Delta D_{wb} + D_{tail} \tag{3.18}$$

$$= \Delta D_{wb} + [D_{tail}]_{datum} + [\Delta D_{tail}]_{trim} \tag{3.19}$$

$$= \Delta D_{wb} + [D_{P_{tail}}]_{datum} + [\Delta D_{P_{tail}} + D_{TV_{tail}}]_{trim}. \tag{3.20}$$

In Equations (3.18) to (3.20) the various terms are as follows.

ΔD_{wb} represents a change in wing-body drag corresponding to a change in wing-body lift to compensate for the tail lift (while retaining constant overall lift). In many cases, particularly for preliminary design calculations, this will be the most significant drag term.

$[D_{P_{tail}}]_{datum}$ is a datum value of tailplane profile drag; this quantity is often assigned to the *airframe* profile drag.

$[\Delta D_{P_{tail}}]_{trim}$ is the change in tailplane profile drag between the datum and trimmed conditions. This term is likely to be ignored in most cases.

$[D_{TV_{tail}}]_{trim}$ is the tailplane trailing vortex drag corresponding to the actual tailplane lift to produce zero resultant moment on the aircraft in the presence of downwash.

The choice of datum is a matter of convenience; three examples are as follows.

(i) The datum is taken as the aircraft at a given wing lift but with zero lift on the tailplane. This corresponds to Equations (3.19) and (3.20) with $\Delta D_{wb} = 0$. It is likely that the contribution $[D_{P_{tail}}]_{datum}$ would be assigned to the airframe profile drag so yielding zero trim drag at the datum condition.

(ii) The datum is taken as the aircraft without its tailplane. This case is represented by Equation (3.19) with $[D_{tail}]_{datum} = 0$ and is particularly relevant where a very wide range of aircraft flight conditions is to be considered – see Addendum G of Reference 32.

(iii) The datum is taken as a standard airframe configuration, centre of gravity position and power setting. In general this involves calculation of the longitudinal trim drag and the wing drag at two sets of conditions but may result in a relatively simple method of representation – see Addendum B of Reference 32.

3.8.5 Treatment of foreplane and close-coupled tail surfaces

The concept of a separate trim drag contribution is of limited value with foreplanes ("canard" configurations) and close-coupled tailplanes – particularly if these are used in conjunction with a low aspect ratio wing. In such cases, for example, it is likely that one design objective will be to achieve a favourable influence on the wing of the trailing vortex sheet from the foreplane – particularly at high angles of attack. (Indeed, in fulfilling such an objective it may even prove necessary to employ additional surfaces (or wing flaps) to obtain a trimmed condition.) For configurations of this type the interdependence of the aerodynamic forces and moments on the various surfaces is such that the isolation of a single contribution offers little advantage.

3.9 Lateral trim drag

Any airframe asymmetry will require some compensating control deflection(s) to maintain zero resultant moment about the yaw and roll axes and there will be a corresponding drag contribution. The topic is dealt with, in effect, in Reference 39 although the main focus there is on the effects of asymmetry in engine thrust.

4. EXAMPLES OF DRAG ESTIMATION METHODS

Tables 6.2 to 6.10 summarise the contributions to airframe drag considered in a number of existing estimation/analysis methods. These are presented in a format based on the Reference Scheme shown in Table 6.1, *i.e.* in terms of a common set of drag component descriptions. The methods considered are from a wide range of sources and represent considerable differences in complexity. In some cases it is possible for simple estimates of drag contributions to be replaced by values deduced from CFD, for example, 2-D aerofoil drag data; 3-D wing-alone or wing-body data. Because of the limited space in the tabular format of the Reference Scheme, the following background notes and References are provided.

Table 6.2, based on Reference 2, is tailored to the prediction of drag on the basis of detailed knowledge of the same manufacturer's previous aircraft. As such it is probably best considered as illustrative of a method for use in those circumstances rather than as one that can be used in isolation.

Table 6.3, based on Reference 4, is a general "project" method intended for use in predicting drag of all airframe components for transport aircraft configurations. While the quality of some of the individual component estimates is uncertain, overall it represents a classic "aerodynamic build-up" procedure.

Table 6.4, based on Reference 6, represents only part of the procedures reported there. The overall purpose of that paper was to identify all the drag prediction/analysis procedures used in the design and development of a particular transport aircraft. In addition to the estimation procedures summarised in Table 6.4, much attention is given to the prediction of drag from wind-tunnel test data and the subsequent comparisons with flight-test. Apart from an estimation of wing drag rise Mach number, all effects of compressibility on drag are derived from tests. In these comparisons it is clear that, as far as profile drag was concerned, the estimates based on the methods summarised in Table 6.4 were no worse than those derived from the wind-tunnel tests.

Table 6.5, based on References 8 and 9, is an empirically-derived method based on test data for a large number of aircraft and wind-tunnel models. These References also form the basis of the estimation method of Reference 49. The primary feature of the method is the provision of incremental values of C_D as departures in C_L and M (including $M>1$) from a datum condition.

Table 6.6, based on Reference 28, is a typical "agreed" set of drag definitions composed for the purposes of making estimates to a common standard throughout the course of a particular set of aircraft project studies. To this purpose it requires a less detailed knowledge of airframe geometry than some other methods but would still provide estimates that were consistent with one another.

Table 6.7, based on Reference 30, is very much biased towards drag at zero lift and is aimed at both subsonic and supersonic applications.

Table 6.8, based on References 17 to 19 and 26, is the first of three "wing-alone" methods that rely on ESDU Data Items and programs. This is the simplest procedure of the three and adopts the classical zero-lift plus drag-due-to-lift contributions.

Table 6.9, based on References 22 to 25, 44, 45, provides a systematic method for the prediction of wing profile drag, including the effects of changes in Mach number and lift coefficient. For vortex drag it relies on the same data as in the method described in Table 6.8.

Table 6.10, based on Reference 38, is the method most closely related to fundamental fluid mechanics principles. The Reference itself is primarily aimed at wave drag prediction for wings but, in validating that method, makes use of procedures for the prediction of viscous and trailing vortex drag that take detailed account of the actual flow about the wing. A consequence of this is that it is the method requiring the greatest degree of information (complete wing pressure distribution) to implement it.

5. REFERENCES

No attempt is made to give a bibliography of methods of predicting aircraft drag. The References in Section 5.1 are those used either in devising the general presentation of the Item or for the Examples of Tables 6.2 to 6.10. The ESDU References quoted in Section 5.2 are those called up specifically in the text of the Item or in Table 6.1. Many more ESDU Items exist on the subject of drag, particularly in the Aerodynamics and Transonic Aerodynamics Series and these are listed in Table 6.11 by their Item number only. See either the ESDU Index or the Location Schedule at the beginning of each Series to identify fully those Items.

5.1 General

1. SQUIRE, H.B. YOUNG, A.D. — The calculation of the profile drag of aerofoils. ARC R & M 1838, 1937.

2. – — Summary and substantiation of aerodynamic data. McDonnell Douglas Corp. Douglas Aircraft Division, Rep. DAC 67124, June 1968.

3. COOKE, J.C. — The drag of infinite swept wings with an addendum. ARC CP 1040, 1969.

4. FINCH, E.C. et al — Drag prediction methods for subsonic airplanes. Boeing Co. Commercial Airplane Division, Report D6–24229, October 1970.

5. GREEN, J.E. WEEKS, D.J. BROOMAN, J.W.F. — Prediction of turbulent boundary layers and wakes in compressible flow by a lag-entrainment method. ARC R & M 3791, January 1973.

6. PATTERSON, J.H. MACWILKINSON, D.G. BLACKERBY, W.T. — A survey of drag prediction techniques applicable to subsonic and transonic aircraft design. Paper No. 1 in *Aerodynamic drag*, AGARD CP-124, October 1973.

7. COOK, T.A. — Measurements of the boundary layer and wake of two aerofoil sections at high Reynolds numbers and high subsonic Mach numbers. ARC R & M 3722, 1973.

8. MORRISON, W.D. JR — Advanced airfoil design empirically based transonic aircraft-drag buildup technique. Lockheed-California Co. NASA CR 137923. See also, by the same author: Empirically based – transonic aircraft – total drag prediction technique – Delta Method. Lockheed California Company report, LR 27027, June 1976.

9. FEAGIN, R.C. MORRISON, W.D. JR — Delta method, a empirical drag buildup technique. Lockheed-California Co., NASA CR 151971, 1978.

10. MIDAP — Guide to in-flight thrust measurement of turbo-jets and fan engines. AGARDograph AG-237, on behalf of the study group of MIDAP (UK Ministry-Industry Drag Analysis Panel), January 1979. (Also available as Report No. 78004 at National Gas Turbine Establishment, Pyestock, 1978.)

11. HUTTON, P.G. *et al* — Guide to drag estimation of aircraft and weapons (U). Procurement Executive, Ministry of Defence, S & T Memo–1–80, November 1980.

12. ASHILL, P.R.
SMITH, P.D.
An integral method for calculating the effects on turbulent boundary-layer development of sweep and taper. RAE TR 83053, June 1983.

13. JOBE, C.E.
Prediction and verification of aerodynamic drag, part 1: prediction. Chapter IV in, *Thrust and drag: its prediction and verification.* Volume 98 in Progress in Astronautics and Aeronautics, AIAA, 1985.

14. LOCK, R.C.
Prediction of the drag of wings at subsonic speeds by viscous/inviscid interaction techniques. In: *Aircraft Drag Prediction and Reduction*. AGARD–R–723, 1985. (See also RAE Tech. Memo. Aero 2077, June 1986).

15. BIL, C.
Development and application of a computer-based system for conceptual aircraft design. Delft University Press, 1988.

16. BOPPE, C.W.
Aircraft drag analysis methods. Paper No. 7 in *Special course on engineering methods in aerodynamic analysis and design of aircraft*. AGARD–R–783, January 1992.

5.2 ESDU Data Items

17. ESDU
Drag of a smooth flat plate at zero incidence. ESDU Data Item Aero W.02.04.01, 1947 (with Amendment B, 1973).

18. ESDU
Profile drag of smooth wings. ESDU Data Item Aero W.02.04.02, 1947.

19. ESDU
Profile drag of smooth aerofoils with straight trailing edges at low speeds. ESDU Data Item Aero W.02.04.03, 1953 (with Amendment A, 1978).

20. ESDU
Approximate estimation of drag of windmilling propellers. ESDU **Performance** Data Item No. ED1/1, April 1962.

21. ESDU
Introduction to the measurement of thrust in flight. ESDU **Performance** Data Item No. 69006, July 1969 (with Amendment A, June 1981).

22. ESDU
Profile drag at the drag-rise condition of aerofoils having a specified form of upper-surface pressure distribution at this condition. ESDU **Aerodynamics** Data Item No. 67011, October 1967 (with Amendment A, October 1973).

23. ESDU
Drag-rise Mach number of aerofoils having a specified form of upper-surface pressure distribution: Charts and comments on design (*supersedes* T.D. Memor. 67009). ESDU **Transonics** Data Item No. 71019, December 1971 (with Amendment A, March 1987).

24. ESDU
Aerofoils having a specified form of upper-surface pressure distribution: Details and comments on design (*supersedes* T.D. Memor. 67010). ESDU **Transonics** Data Item No. 71020, December 1971 (with Amendment A, October 1973).

25. ESDU — Adaptation of drag rise charts in T.D. Memo 71019 to the mid-semi-span portion of swept and tapered planforms. ESDU **Transonics** Data Item No. 72027, November 1972.

26. ESDU — Subsonic lift-dependent drag due to the trailing vortex wake for wings without camber or twist. ESDU **Aerodynamics** Data Item No. 74035, 1974.

27. ESDU — A framework relating the drag-rise characteristics of a finite wing/body combination to those of its basic aerofoil. ESDU **Transonics** Data Item No. 78009, May 1978.

28. – — Format and assumptions for high speed drag estimation. Joint Technical Team, “Group of Six”, Weybridge, February 1976.

29. ESDU — Undercarriage drag prediction methods. ESDU **Aerodynamics** Data Item No. 79015, September 1979 (with Amendments A and B, March 1987).

30. – — Unpublished Report, 1980.

31. ESDU — Estimation of windmilling drag and airflow of turbo-jet and turbo-fan engines. ESDU **Performance** Data Item No. 81009, June 1981 (with Amendment A, April 1984).

32. ESDU — Representation of drag in aircraft performance calculations. ESDU **Performance** Data Item No. 81026, September 1981 (with Amendments A to C, July 1997).

33. ESDU — Drag of axisymmetric cowls at zero incidence for subsonic Mach numbers. ESDU **Aerodynamics** Data Item No. 81024, November 1981 (with Amendment A, December 1994).

34. ESDU — Estimation of spillage drag for a wide range of axisymmetric intakes at $M < 1$. ESDU **Performance** Data Item No. 84004, April 1984 (with Amendment A, June 1984).

35. ESDU — Estimation of drag due to inoperative turbo-jet and turbo-fan engines using Data Item Nos 81009 and 84004. ESDU **Performance** Data Item No. 84005, July 1984 (with Amendment A, March 1989).

36. ESDU — Introduction to installation effects on thrust and drag for propeller-driven aircraft. ESDU **Aerodynamics** Data Item No. 85015, June 1985.

37. ESDU — Thrust and drag accounting for propeller/airframe interaction. ESDU **Aerodynamics** Data Item No. 85017, November 1985.

38. ESDU — A method of determined the wave drag and its spanwise distribution on a finite wing in transonic flow (supersedes T.D. Memor. 83022). ESDU **Transonics** Data Item No. 87003, April 1987 (with Amendment B, February 1995).

39. ESDU — Estimation of drag arising from asymmetry in thrust or airframe configuration. ESDU **Performance** Data Item No. 88006, December 1988 (with Amendment A, September 1989).

40. ESDU — Introduction to transonic aerodynamics of aerofoils and wings. ESDU **Transonics** Data Item No. 90008, April 1990.

41. ESDU — Wave drag coefficient for axisymmetric forecowls at zero incidence. ESDU **Transonics** Data Item No. 94014, June 1994.

42. ESDU — Excrescence drag levels on aircraft. ESDU **Performance** Data Item No. 94044, November 1994.

43. ESDU — Drag due to lift for plane swept wings, alone or in combination with a body, up to high angles of attack at subsonic speeds. ESDU **Aerodynamics** Data Item No. 95025, November 1995 (with Amendment A, December 1997).

44. ESDU — VGK method for two-dimensional aerofoil sections, Part 1: Principles and results. ESDU **Transonics** Data Item No. 96028, October 1996.

45. ESDU — VGK method for two-dimensional aerofoil sections, Part 2: User manual for operation with MS-DOS and UNIX systems. ESDU **Transonics** Data Item No. 96029, October 1996.

46. ESDU — Drag due to lift for non-planar swept wings up to high angle of attack at subsonic speeds. ESDU **Aerodynamics** Data Item No. 96025, April 1997.

47. ESDU — Guide to wing aerodynamic design. ESDU **Transonics** Data Item No. 97017, August 1997.

48. ESDU — Similarity rules for application in aircraft performance work. ESDU **Performance** Data Item No. 97025, September 1997.

49. ESDU — Estimation of drag for a wide range of aircraft types. ESDU **Performance** Data Item to be issued.

6. TABLES

TABLE 6.1 CONTRIBUTIONS TO AIRFRAME DRAG: REFERENCE SCHEME

	Notation	Interpretation/Comments	
1.	D	$= D_F + D_{PR}$ $= D_P + D_{TV} + D_W$ } See Sketch 3.1	
2.	C_{Ldatum} M_{datum} Re_{datum}	Datum conditions *sometimes* used to specify flight conditions of main interest and/or to simplify calculations to form: [datum drag] + [increment(s) due to change(s) from datum conditions].	
3.	D_P Profile drag (a)	Major airframe components: wing, body, tail, pylons, cowls, flaptracks.	Primary effect of boundary layer growth; may be subdivided into skin friction and pressure (form) elements. Wave drag for $M<1$ usually included here.
	(b)	Misc. airframe components: *e.g.* canopy, "blisters", fuselage, upsweep, base area (non-propulsive).	
	(c)	Excrescences: includes surface joints, gaps, leaks, internal flow, aerials – see Section 3.3.	
	(d)	Interference effects on profile drag – may include wave-drag elements at $M<1$.	
	(e)	Propulsion system drag contributions: spillage, afterbody/base, windmilling engines or propellers.	
4.	$[\Delta D_P]_{\Delta C_L}$ $[\Delta D_P]_{\Delta M}$ $[\Delta D_P]_{\Delta Re}$	Terms to represent change(s) in D_P due to change from datum conditions, see item 1 above.	
5.	D_{TV} Trailing vortex drag	Includes effect of body on wing flow, but excludes trim drag.	Some (older) methods redefine these terms to include the variations with C_L of profile drag, see item 4 above.
6.	$\Delta[D_{TV}]_{\Delta C_L}$ $\Delta[D_{TV}]_{\Delta M}$ $\Delta[D_{TV}]_{\Delta Re}$	Terms to represent changes in D_{TV} due to change from datum conditions.	
7.	D_W Wave drag	For $M>1$ this is treated as a separate item but for $M<1$ it may be treated as a part of item 3.	
8.	D_{trim}	Longitudinal trim drag.	
9.	$D_{asym\ thr}$	Directional trim drag, see Data Item No. 88006, Reference 39.	These topics are not dealt with in this Data Item.
10.	D_{uc}	Undercarriage drag, see Data Item No. 79015, Reference 29.	
11.	D_{stores}		
12.	Drag of high-lift devices	(a) Take-off and landing (b) Manoeuvres } See Table 6.11.	

TABLE 6.2 CONTRIBUTIONS TO AIRFRAME DRAG: EXAMPLE BASED ON REFERENCE 2

	Notation (Reference scheme)		Summary of estimation method based on Reference 2
1.	D		$= D_0 + D_i + D_W$ "parasite" + "lift induced" + "compressibility" (Reference 2 terms).
2.	C_{Ldatum} M_{datum} Re_{datum}		$C_L = 0$ $M = 0.5$ Taken as Re for cruise.
3.	D_P Profile drag	(a), (b)	Zero lift "parasite" drag estimated for all airframe components using form factors and skin friction at datum conditions. (Nacelles assigned to thrust account, not drag). Form factors presumed to account for all aspects of pressure drag including separations. For wing $\lambda = 1 + Z(t/c) + 100(t/c)^4$ with $Z = 2$ for $\Lambda = 0$; $Z = 1.4$ for $\Lambda = 35°$.
		(c)	Control surface gaps treated separately. All other excrescences treated as value of C_{Fe} based on Company experience.
		(d)	Interferences estimated separately for wing/pylon/nacelle, fuselage/nacelle.
		(e)	No propulsion-system related drag terms.
4.	$[\Delta D_P]_{\Delta C_L}$ $[\Delta D_P]_{\Delta M}$ $[\Delta D_P]_{\Delta Re}$		All effects treated in item 5 Estimated as indicated at item 7 Evaluated using skin friction law.
5.	D_{TV} Trailing vortex drag		"Induced" drag deduced using $C_{D_i} = C_L^2 / \pi Ae$. Value of e estimated in two parts: (i) Theoretical vortex drag increment due to non-elliptic loading, fuselage interference, wing planform and twist. (ii) Empirical method for variation of parasite drag with lift, based on previous aircraft.
6.	$[\Delta D_{TV}]_{\Delta C_L}$ $[\Delta D_{TV}]_{\Delta M}$ $[\Delta D_{TV}]_{\Delta Re}$		Implicit in method of item 5 None None.
7.	D_W	$M < 1$	"Compressibility" drag given by $C_{DW}/\cos^3\Lambda_{¼} = f[M/M_{crit,\,crest}]$ where $M_{crit,\,crest}$ is flight M for sonic velocity at wing crest; values obtained from flight test.
		$M > 1$	Not considered.
8.	D_{trim}		Not considered separately; presumed to be included in item 5 which includes empirical data for "trimmed" aircraft.

TABLE 6.3 CONTRIBUTIONS TO AIRFRAME DRAG:
EXAMPLE BASED ON REFERENCE 4

	Notation (Reference scheme)		Summary of estimation method based on Reference 4
1.	D		$= D_P + D_{TV} + D_W + D_{trim}$ "parasite" + "vortex" + "drag rise" + "trim drag" (Reference 4 terms).
2.	C_{Ldatum} M_{datum} Re_{datum}		None M_I, denoting "incompressible" conditions with M_I = f[$\Lambda_{¼}$] None.
3.	D_P Profile drag	(a), (b)	"Parasite" drag (at M_I) estimated for all airframe components for range of C_L values and at least two values of Re (initial and final cruise) using skin friction and form factors. For aerodynamic surfaces, separate factors apply for effects of thickness, camber and sweep (based on simple sweep theory using $\Lambda_{¼}$). For body, factors allow for fineness ratio, upsweep and aft end closure (plan view). For nacelles factors allow for fineness ratio, mass flow ratio and (aft-end) separation. For pylons, factor accounts for thickness. Several miscellaneous items considered.
		(c)	Excrescence drag taken as fraction of D_P that varies with S_{wet} for aircraft.
		(d)	Interference factors given for wing/body, tail/body, fin/body, body/nacelle, wing/nacelle.
		(e)	Propulsion system terms included in (b) and (d); scrubbing drag evaluated separately.
4.	$[\Delta D_P]_{\Delta C_L}$ $[\Delta D_P]_{\Delta M}$ $[\Delta D_P]_{\Delta Re}$		Form factors for camber and aft-fuselage upsweep vary with C_L See Item 7 See Item 3(a).
5.	D_{TV} Trailing vortex drag		Estimated as $C_{D_{TV}} = KC_L^2/\pi A$. Values of K given as f[$(d/b)^2$, factors to account for non-elliptic loading].
6.	$[\Delta D_{TV}]_{\Delta C_L}$ $[\Delta D_{TV}]_{\Delta M}$ $[\Delta D_{TV}]_{\Delta Re}$		Implicit in method for D_{TV} None (but see items 7 and 8) None.
7.	D_W	$M<1$	"Drag rise" Wing: For each C_L value (see item 3(a)), M_{crit} estimated (at which C_D is 0.002 greater than value at M_I) ; M_{crit} = f [(technology level, sweep, thickness, camber)]. Standard curve shapes used for $M \le M_{crit}$. Body: D_W/q = f [(M, forebody fineness ratio)] Tail: D_W/q = f [(thickness, sweep)] Trim: Change in wing lift due to trimming affects M_{crit} and hence wing D_W.
		$M>1$	Not considered.
8.	D_{trim}		Estimate assumes trim drag can be "tailored" to small value; simple method then gives D_{trim}/q = f[C_L, "design C_L"]. Better estimate given as function of wing and tail lift coefficients, downwash and vortex drag characteristics. See also item 7.

TABLE 6.4 CONTRIBUTIONS TO AIRFRAME DRAG: EXAMPLE BASED ON REFERENCE 6

	Notation (Reference scheme)		Summary of estimation method based on Reference 6
1.	D		$= D_P + D_{TV} + D_{trim}$ but see Section 4.
2.	C_{Ldatum} M_{datum} Re_{datum}		} None.
3.	D_P Profile drag	(a), (b)	Wing: strip theory (Section 3.3.2) used with aerofoil data taken from: (i) Combination of skin friction and form factors (*e.g.* References 18, 19) for minimum value and empirical relationship for variation of $[C_{D_P}]_n$ with lift coefficient. (ii) Aerofoil measured data. (iii) Two-dimensional flow code (iterative solution for potential outer flow and boundary-layer model). Bodies: Preliminary estimates based on simple correlation using skin friction and form factors related to an effective fineness ratio. Tail surfaces: treated as wing (see also item 8). Nacelles: estimates based on skin friction with allowance for spillage and afterbody drag terms.
		(c)	Excrescences: detailed estimates for use with wind tunnel data; flap tracks assigned to excrescences.
		(d)	Interference: At preliminary stage all effects on D_P taken as negligible – to be achieved by filleting at wind-tunnel test stage.
		(e)	Propulsion system: Nacelle-alone drag assigned to thrust account; pylons and interference to airframe (data derived from tunnel tests).
4.	$[\Delta D_P]_{\Delta C_L}$ $[\Delta D_P]_{\Delta M}$ $[\Delta D_P]_{\Delta Re}$		Variations in D_P due to changes in C_L and Re are implicit in the methods in item 3. See item 7 and Section 4 regarding effects of Mach number.
5.	D_{TV} Trailing vortex drag		Deduced from computed spanwise loading for complete wing/body combination (lifting-surface, vortex lattice and linearised methods). See Table 6.9 for example of similar procedure.
6.	$[\Delta D_{TV}]_{\Delta C_L}$ $[\Delta D_{TV}]_{\Delta M}$ $[\Delta D_{TV}]_{\Delta Re}$		} All variations in D_{TV} are implicit in the method of item 5.
7.	D_W	$M<1$	No values calculated (but see Section 4). Wing drag rise Mach number estimated using strip integration (item 3) while allowing aerofoil data to reach drag-rise condition at single spanwise station.
		$M>1$	Not considered.
8.	D_{trim}		Estimated as in Equation (3.20) with $[D_{Ptail}]_{datum}$ assigned to D_P (*i.e.* item 3).

TABLE 6.5 CONTRIBUTIONS TO AIRFRAME DRAG: EXAMPLE BASED ON REFERENCES 8 AND 9

	Notation (Reference scheme)	Summary of estimation method based on References 8 and 9
1.	D	$C_D = C_{D_{min}} + C_{D_i}$ $C_{D_{min}} = C_{D_{Pmin}} + [\Delta C_{D_P}]_{\Delta M} + C_{D_{misc}}$ $C_{D_i} = C_{D_{TV}} + \Delta C_{D_{PR}}$
2.	C_{Ldatum} M_{datum} Re_{datum}	} Values estimated corresponding to $0.99(ML/D)_{max}$; referred to as design conditions. Based on cruise height and speed.
3.	D_P (a), (b) Profile drag	Contributions to $C_{D_{Pmin}}$ for each airframe component estimated from skin friction, wetted area and form factors – see Section 3.3.1. Values of "wave drag due to volume" calculated as in item 4.
	(c)	Excrescence drag effects estimated as simple fraction of $C_{D_{Pmin}}$
	(d), (e)	Presumed to be included in $C_{D_{Pmin}}$ or $[\Delta C_{D_P}]_{\Delta M}$ (see item 4).
4.	$[\Delta D_P]_{\Delta C_L}$ $[\Delta D_P]_{\Delta M}$ $[\Delta D_P]_{\Delta Re}$	None; see item 6. Values of "wave drag due to volume" estimated empirically as function $(M - M_{datum})$. Effect of changes from Re_{datum} estimated as simple factor giving skin friction variation with Mach number.
5.	D_{TV} Trailing vortex drag	Estimated as $C_{D_i} = C_{D_{TV}} + \Delta C_{D_{PR}}$ $= \frac{C_L^2}{\pi A} + \Delta C_{D_{PR}}$. Values of $\Delta C_{D_{PR}}$ estimated empirically as functions of $(C_L - C_{L_{datum}})$, $(M - M_{datum})$.
6.	$[\Delta D_{TV}]_{\Delta C_L}$ $[\Delta D_{TV}]_{\Delta M}$ $[\Delta D_{TV}]_{\Delta Re}$	See item 5 See item 5 None.
7.	D_W $M<1$ $M>1$	Wave drag is included in the quantities $[\Delta C_{D_P}]_{\Delta M}$ and $\Delta C_{D_{PR}}$ estimated empirically in items 4 and 5.
8.	D_{trim}	Not estimated separately; presumed to be included in items 5 and 6 which are based on flight data for "trimmed" aircraft.

TABLE 6.6 CONTRIBUTIONS TO AIRFRAME DRAG: EXAMPLE BASED ON REFERENCE 28

	Notation (Reference scheme)		Summary of estimation method based on Reference 28
1.	D		$D_0 + D_i + D_W$ "zero lift" + "induced" + "compressibility" (Reference 28 terms)
2.	C_{Ldatum} M_{datum} Re_{datum}		$C_L = 0$ None Based on $V\rho/\mu = 7\times10^6$ (m^{-1}) (2.13×10^6 (ft^{-1})).
3.	D_P Profile drag	(a), (b)	Contributions to D_0 estimated for each airframe component at datum value of Re using skin friction, form factors and wetted areas. Wing: λ values function of aerofoil type, thickness and sweep. Body: λ values function of fineness ratio and cross-section shape. Fin, tail: values estimated as for wing. Nacelles: λ values function of mass flow ratio and ratio of inlet to maximum diameter. Pylons: λ values taken from aerofoil data. Flap tracks: λ value taken as constant; size taken as constant fraction of reference wing area.
		(c)	Excrescence drag taken as constant fraction of D_0.
		(d)	Interference drags estimated separately as follows: Body/ wing/ flap tracks: Constant fraction of D_0 for those components. Fin/ tail: Constant fraction of tailplane D_0 plus contribution dependent on number of junctions. Nacelle/ wing: Fixed vertical position of cowl assumed; factor on cowl D_0 depends on nacelle and wing longitudinal dimensions.
4.	$[\Delta D_P]_{\Delta C_L}$ $[\Delta D_P]_{\Delta M}$		} All effects of C_L and M changes are taken into account in items 5 and 7.
	$[\Delta D_P]_{\Delta Re}$		Variations in skin friction estimated separately for each airframe component for changes from Re_{datum}.
5.	D_{TV} Trailing vortex drag		"Induced" drag estimated as $C_{D_i} = KC_L^2/\pi A$. Values of K based on test data for previous aircraft adjusted to take account of aspect ratio and operating value of C_L and M.
6.	$[\Delta D_{TV}]_{\Delta C_L}$ $[\Delta D_{TV}]_{\Delta M}$		} implicit in method of item 5.
	$[\Delta D_{TV}]_{\Delta Re}$		None.
7.	D_W	$M<1$	"Compressibility": drag rise Mach number taken as function of C_L. Values of C_{D_W} estimated as function of increment in M above drag-rise value.
		$M>1$	Not considered.
8.	D_{trim}		Not considered separately since method of item 5 based on flight data for "trimmed" aircraft.

TABLE 6.7 CONTRIBUTIONS TO AIRFRAME DRAG: EXAMPLE BASED ON REFERENCE 30

	Notation (Reference scheme)		Summary of estimation method based on Reference 30
1.	D		$= D_0 + D_i$ Method primarily directed to "zero-lift" drag, D_0 (Reference 30 term).
2.	C_{Ldatum} M_{datum} Re_{datum}		$C_L = 0$ $M = 0.8$ Based on flight at $M = 0.8$.
3.	D_P Profile drag	(a)	Contributions to (subcritical) value of "zero-lift" drag, expressed as D_0/q, estimated using incompressible skin friction, form factors and wetted areas. Skin friction values used take account of small scale surface roughness and are evaluated for effective mean chord. Aerodynamic surfaces: λ values functions of thickness and sweep. Fuselage: skin friction calculations $(\lambda = 1)$ take account of different starting points (nose and intake lips) for different parts of boundary layer. Drag due to fuselage shape accounted for as afterbody/base effects estimated using areas of maximum cross section, base and nozzle exit.
		(b)	Miscellaneous features: λ values derived to represent geometry and location of feature.
		(c)	Excrescences: represented as fractions of individual contributions to D_0/q
		(d)	Interference: not considered separately
		(e)	Propulsion system: Boundary-layer diverter: contribution to D_0/q taken as fraction of diverter frontal area. Base drag: see item 3(a).
4.	$[\Delta D_P]_{\Delta C_L}$ $[\Delta D_P]_{\Delta M}$ $[\Delta D_P]_{\Delta Re}$		None See item 7 Skin friction calculations adjusted for $M \neq 0.8$.
5.	D_{TV} Trailing vortex drag		$C_{D_i} = K_1 C_L^2$ for $C_L < C_{L_{crit}}$ $= K_1 C_{L_{crit}}^2 + K_2 (C_L^2 - C_{L_{crit}}^2)$ for $C_L > C_{L_{crit}}$.
6.	$[\Delta D_{TV}]_{\Delta C_L}$ $[\Delta D_{TV}]_{\Delta M}$ $[\Delta D_{TV}]_{\Delta Re}$		Implicit in method of item 5 None None.
7.	D_W	$M < 1$	Drag-rise M estimated as function of ratio of wing sweep to thickness. At drag-rise condition $[\Delta C_{D_0}]_{\Delta M} = 0.002$ and $dC_{D_0}/dM = 0.001$. Standard curves used to define variation from incompressible value, through drag rise to $M = 1$ and beyond.
		$M > 1$	Aerodynamic surfaces: Contribution to D_W/q calculated as function of M and an effective thickness/chord ratio which itself depends on aspect ratio, sweep and thickness. Fuselage: Contribution to D_W/q calculated separately for fore- and afterbody as functions of M and equivalent fineness ratios.
8.	D_{trim}		Not considered.

**TABLE 6.8 CONTRIBUTIONS TO AIRFRAME DRAG:
EXAMPLE BASED ON REFERENCES 17 TO 19 AND 26 (WING ALONE)**

	Notation (Reference scheme)		Summary of estimation method based on References 17 to 19 and 26
1.	D		$D_P + D_{TV}$
2.	C_{Ldatum} M_{datum} Re_{datum}		$C_L = 0$ $M \equiv 0$, as method relates to incompressible flow Re chosen to suit application.
3.	D_P Profile drag		Profile drag coefficient at $C_L = 0$ evaluated using strip method of Equation (3.12) using sweep angle $\Lambda_{¼}$ or $\Lambda_{½}$. Skin friction values taken from Reference 17; aerofoil form factors from References 18, 19. For unswept wings, the strip method could be replaced by simpler procedure treating wing as single element with average values taken for wing planform and section properties.
4.	$[\Delta D_P]_{\Delta C_L}$ $[\Delta D_P]_{\Delta M}$ $[\Delta D_P]_{\Delta Re}$		See Item No. 66032 None Considered through effect of skin friction.
5.	D_{TV} Trailing vortex drag		Estimated using method of Equation (3.16) and values of $(1+\delta)$ from Reference 26.
6.	$[\Delta D_{TV}]_{\Delta C_L}$ $[\Delta D_{TV}]_{\Delta M}$ $[\Delta D_{TV}]_{\Delta Re}$		Considered through Equation (3.16); method not applicable at $C_L > C_{L_{crit}}$ None None.
7.	D_W	$M<1$	Not considered.
		$M>1$	Not considered.
8.	D_{trim}		Not considered; method is for wing alone.

TABLE 6.9 CONTRIBUTIONS TO AIRFRAME DRAG: EXAMPLE BASED ON REFERENCES 22 TO 25, 44, 45

	Notation (Reference scheme)	Summary of estimation method based on References 22 to 25, 44, 45
1.	D	$= D_P + [\Delta D_P]_{\Delta C_L} + [\Delta D_P]_{\Delta M} + D_{TV}$
2.	C_{Ldatum} M_{datum} Re_{datum}	} Taken as values corresponding to the drag-rise condition C_{L_D}, M_D for the aerofoil family given in References 22 to 24. None.
3.	D_P Profile drag	Profile drag at the datum (drag-rise) condition estimated using strip method of Equation (3.11). Those conditions are defined in Ref. 23; values of $\left[C_{D_{P_n}}\right]_{datum}$ are given in Reference 22. Values of "effective sweep angles", Λ_e, for use in this method are given in Item No. 72027 (Reference 25). Aerofoil geometries are given in Reference 24. (The method can be applied with any systematic set of aerofoil data.)
4.	$[\Delta D_P]_{\Delta C_L}$ $[\Delta D_P]_{\Delta M}$ $[\Delta D_P]_{\Delta Re}$	Effects of changes in C_L and M for the particular family of aerofoils (or any other family) can be generated using the VGK aerofoil method of References 44, 45.
5.	D_{TV} Trailing vortex drag	Estimated using method of Equation (3.16) and values of $(1+\delta)$ from Reference 26.
6.	$[\Delta D_{TV}]_{\Delta C_L}$ $[\Delta D_{TV}]_{\Delta M}$ $[\Delta D_{TV}]_{\Delta Re}$	Considered through Equation (3.16); method not applicable at $C_L > C_{L_{crit}}$ None None.
7.	D_W $M<1$	Wave drag is accounted for $(M<1)$ by the incremental effects on profile drag due to C_L and M changes from the datum.
	$M>1$	Not considered.
8.	D_{trim}	Not considered; method is for wing alone.

TABLE 6.10 CONTRIBUTIONS TO AIRFRAME DRAG: EXAMPLE BASED ON REFERENCE 38 (WING ALONE)

	Notation (Reference scheme)	Summary of estimation method based on Reference 38
1.	D	$= D_V + D_{TV} + D_W$
2.	C_{Ldatum} M_{datum} Re_{datum}	No datum conditions. Drag components evaluated at each combination of values of C_L, M, Re.
3.	D_P Profile drag	The surface pressures on both wing surfaces are used as input to an infinite tapered wing version[12] of the RAE lag entrainment boundary-layer method[5] that allows for sweep and taper effects on the boundary-layer development on the assumption that the spanwise variation of the pressure distribution is small. This calculation yields the momentum thicknesses of the boundary layers at the trailing edge on both upper and lower surfaces. The corresponding values of momentum thickness at downstream infinity are calculated using the Squire and Young technique[1] with appropriate modifications for the effects of compressibility[7] and trailing-edge sweep[3]. Integrating the viscous drag contributions across the span yields the total viscous drag coefficient.
4.	$[\Delta D_P]_{\Delta C_L}$ $[\Delta D_P]_{\Delta M}$ $[\Delta D_P]_{\Delta Re}$	Each drag component is evaluated separately, from a knowledge of wing surface pressures, at the particular combinations of values of C_L, M, Re.
5.	D_{TV} Trailing vortex drag	The vortex drag coefficient is estimated by a Trefftz-plane calculation using as input the spanwise load distribution obtained by integrating the measured chordwise pressure distributions to get the local lift coefficients and assuming that the load carries over smoothly across the body.
6.	$[\Delta D_{TV}]_{\Delta C_L}$ $[\Delta D_{TV}]_{\Delta M}$ $[\Delta D_{TV}]_{\Delta Re}$	Each drag component is evaluated separately from a knowledge of wing surface pressures at the particular combination of values of C_L, M, Re.
7.	D_W $M<1$	The wave drag coefficient at a local spanwise station, η, of a finite wing is given as a function of M, Λ_{sh}, M_{Lnsh} and $\bar{\kappa}$ where M_{Lnsh} is the local Mach number ahead of the shock(s) and $\bar{\kappa}$ is the mean surface curvature of a streamwise section in the vicinity of the shock. The total wave drag coefficent of the wing is given by $C_{DW} = \int_{\eta_{body\ side}}^{1} \frac{c(\eta)}{\bar{c}} C_{DW}(\eta) d\eta$. All flow properties required are deduced from chordwise distributions of C_P at each local spanwise station.
	$M>1$	Not considered.
8.	D_{trim}	Not considered; method is for wing alone.

FLAT PLATES (ALONG, NORMAL TO AND AT INCIDENCE TO FLOW)		
Boundary – layer skin friction smooth surface, laminar smooth surface, turbulent rough surface, turbulent	also applicable to wedges cylinders cones	68019 68020 73016
Limits for laminar flow surface waviness on wings grain size on wings or bodies		 W.02.04.11 W.02.04.09
Wave drag, blunt leading edge Total drag, finite plates normal to and at incidence to flow		W.S.02.03.10 70015

AEROFOILS	
Drag components independent of lift incompressible flow	W.02.04.00 W.02.04.01 W.02.04.02 W.02.04.03 W.02.04.09 W.02.04.11
$M > 1$ (zero wave drag)	W.S.02.04.12 W.S.02.04.13
Wave drag, $M > 1$ (including effect of lift)	W.S.00.03.03 W.S.00.03.04 W.S.00.03.05
Base pressure with blunt trailing edge, $M > 1$	W.S.02.03.07
Estimation of critical M	W.00.03.01 74008
Estimation of drag-rise M	TDM 6407*
Particular family of aerofoils: profile drag at drag rise drag-rise conditions aerofoil designs	 67011 71019* 71020*
VGK aerofoil method (with or without plain flaps)	96028* 96029*

FLAPS	
Drag component independent of lift full-span plain flap full-span, single-slotted flap full-span split flap effect of flap span effect of fuselage	 87024 87005 74010 F.02.01.07 97003
Lift-dependent component of drag part-span flap part-span flap with central cut out	 F.02.01.08 F.02.01.08
Interference between jet efflux and slotted flap	82034

WINGS	
Drag components independent of lift Wave drag, transonic M wave drag, $M > 1$	 W.S.02.03.09 75004
Lift-dependent components of drag	95025 96025
subcritical M trailing vortex drag, $M < 1$ $M > 1$ two staggered lifting surfaces at low speeds	66031, 66032 74035 W.S.02.03.02 81023
Total drag of slender wings at low speeds	71006
Drag-rise characteristics – relationship between wing/body combination and basic aerofoil	78009*
Wave drag (and spanwise distribution) on finite wing in transonic flow	87003*

GROUND EFFECT	
Aircraft at low speed	72023

SPOILERS (LIFT DUMPERS)	
drag increment drag during ground run	96026 76026

OTHER MAJOR AIRFRAME AND MISCELLANEOUS COMPONENTS	
Optimum area distribution and wave drag at transonic M (area rule)	A.S.02.03.01 A.02.03.02
Rear-fuselage upsweep	80006
Canopies (fighter-type)	67041
Undercarriages	79015
Parachutes	85029†
Wave drag, $M > 1$ rectangular planform fairings	 71018

AXISYMMETRIC BODIES DRAG INDEPENDENT OF LIFT (*i.e.* axial flow)	
Bodies with pointed tails, subcritical M	78019
Blunt forebodies, $0 < M < 4$	80021
Blunt conical forebody, $M > 1$	68021 82028
Conical boat-tails (afterbodies)	
base drag, $M < 1$	76033
boat-tail pressure drag, $M < 1$	77020
base and boat-tail pressure drag, transonic M	78041
base drag, $M > 1$	79022
Circular-arc boat-tails (afterbodies)	
base and boat-tail pressure drag	96012
effect of incidence	96033
Drag-rise Mach number: smooth or bumpy bodies	74013*
Wave drag, forebodies, transonic M	79004* 83017* 89033*
Wave drag, $M > 1$	B.S.02.03.01
ducted forebodies, truncated afterbodies	B.S.02.03.02
forebody-afterbody interference, pointed or ducted bodies	B.S.02.03.08

EXCRESCENCES	
Total drag increments for	
circular cavities	74036
grooves	75028
two-dimensional steps, ridges	75031
spherically-headed rivets	76008
Circular cylinder(s) normal to flat plate	83025
Stub wings and fairings	84035
Auxiliary inlets	86002
Control gaps	92039
Vortex generators	93024* 93025*
Excrescence drag magnification	87004* 91028 91029
Example for wing	93032
Overall aircraft levels of excrescence drag	94044†

POWERPLANT – RELATED DRAG	
NACA – 1 Series cowls	81024
Forecowl wave drag $0.6 \leq M \leq 1.4$	94014*
Inoperative turbo-jet and turbo-fan engines (using 81009 and 84004)	84005†
Windmilling jet and fan engines	81009†
Spillage drag, all axisymmetric intakes, $M < 1$	84004†
Drag due to thrust (or airframe) asymmetry	88006†
Propeller interactions	85015 85017 86017 88031
Windmilling propellers	ED1/1†

BODIES (NON-STREAMLINE)	
Infinite cylinders	
circular section	80025
polygonal and elliptical sections	79026
Finite cylinders	
circular section	81017
Rectangular blocks	71016
Rectangular prisms, surface mounted, in turbulent shear flow	80003

TABLE 6.11

GUIDE TO COMPONENT DRAG DATA IN OTHER ITEMS AND SERIES

No Superscript indicates Item from ESDU Aerodynamics Series.
* indicates Item from ESDU Transonic Aerodynamics Series.
† indicates Item from ESDU Performance Series.

THE PREPARATION OF THIS DATA ITEM

The work on this particular Data Item was monitored and guided by the Performance Committee, which first met in 1946 and now has the following membership:

Chairman
Mr K.J. Balkwill – Independent

Vice-Chairman
Mr W.L. Horsley – Civil Aviation Authority, Safety Regulation Group

Members
Mr P.V. Aidala* – Northrop Grumman ESID, Bethpage, NY, USA
Mr T. Bartup – Avro International Aerospace, Woodford
Mr E.N Brailsford – Independent
Mr M.Broad – Independent
Mr G.M.J. Davis – DERA, Boscombe Down
Mr N.J. Herniman – Airbus Industrie, Toulouse, France
Mr R.G. Humpston – Rolls-Royce plc, Aero Division, Derby
Mr T.S.R. Jordan – Independent
Mr R.J. Orlowski* – Boeing Commercial Airplane Company, Seattle, Wash., USA
Dr P. Render – Loughborough University
Mr P. Robinson – Independent
Mr D.N. Sinton – Independent
Mr G.J.R. Skillen – Civil Aviation Authority, Safety Regulation Group
Mr G.E. Smith – Independent
Mr A. Stanbrook – Independent
Mr R. Storey – British Aerospace Defence Ltd, Brough
Prof. E. Torenbeek* – Delft University of Technology, Holland
Mr Y.D. Traeger* – Israel Aircraft Industies, Jerusalem, Israel
Mr C.J. Turner* – McDonnell Douglas, Long Beach, Calif., USA
Mr M. Wilson – Pilatus Britten Norman, Isle of Wright
Mr R.D. Younger* – Raytheon Aircraft Company, Wichita, USA

* Corresponding Member

The technical work involved in the initial assessment of the available information and the construction and subsequent development of the Data Item was carried out by,

Mr D.J. Mitchell – Group Head.

The person with overall responsibility for the work in this subject area is Mr D.J. Mitchell.